The Araucaria Project: Distance to the Local Group Galaxy NGC 3109 from Near-Infrared Photometry of Cepheids[1]

I. Soszyński

Universidad de Concepción, Departamento de Fisica, Casilla 160–C, Concepción, Chile
Warsaw University Observatory, Al. Ujazdowskie 4, 00-478 Warszawa, Poland

soszynsk@astrouw.edu.pl

W. Gieren

Universidad de Concepción, Departamento de Fisica, Casilla 160–C, Concepción, Chile

wgieren@astro-udec.cl

G. Pietrzyński

Universidad de Concepción, Departamento de Fisica, Casilla 160–C, Concepción, Chile
Warsaw University Observatory, Al. Ujazdowskie 4, 00-478 Warszawa, Poland

pietrzyn@astro-udec.cl

F. Bresolin

Institute for Astronomy, University of Hawaii at Manoa, 2680 Woodlawn Drive, Honolulu HI 96822, USA

bresolin@ifa.hawaii.edu

R.-P. Kudritzki

Institute for Astronomy, University of Hawaii at Manoa, 2680 Woodlawn Drive, Honolulu HI 96822, USA

kud@ifa.hawaii.edu

and

J. Storm

Astrophysikalisches Institut Potsdam, An der Sternwarte 16, D-14482 Potsdam, Germany

jstorm@aip.de

ABSTRACT

We present near-infrared J- and K-band photometry of 77 Cepheid variables in the Local Group galaxy NGC 3109. Combining our data with the previously published optical V- and I-band photometry of Cepheids in this galaxy we derive an accurate distance and interstellar reddening to NGC 3109. Adopting a distance modulus of 18.5 mag for the Large Magellanic Cloud, we obtain a true distance modulus to NGC 3109 of $(m - M)_0 = 25.571 \pm 0.024$ mag (random error), corresponding to a distance of 1.30 ± 0.02 Mpc. The systematic uncertainty on this value (apart from the adopted LMC distance) is of the order of $\pm 3\%$, the main contributors to this value being the uncertainty on the photometric zero points, and the effect of blending with unresolved companion stars. The total reddening determined from our multiwavelength solution is $E(B-V) = 0.087 \pm 0.012$ mag. About half of the reddening is produced internal to NGC 3109. Our distance result is consistent with previous determinations of the distance to NGC 3109, but has significantly reduced error bars.

Subject headings: stars: Cepheids — distance scale — galaxies: distances and redshift — galaxies: individual (NGC 3109) — infrared: stars

1. Introduction

The effectiveness of using multiwavelength optical and near-infrared (NIR) observations of Cepheids for determining extragalactic distances has been known for years (McGonegal et al. 1982; Madore & Freedman 1991). However, only recently the technical problems with obtaining reliable NIR photometry of faint objects in dense regions have been solved. Using NIR photometry of the Cepheids provides a number of advantages. First, the total and differential reddening is significantly reduced in comparison with the optical bandpasses. Second, the width of the Cepheid period–luminosity (PL) relation is decreasing toward longer wavelengths. Third, NIR photometry of Cepheids is thought to be less sensitive to eventual metallicity effects than optical photometry. Fourth, the amplitudes of variability are significantly smaller in the NIR than in the optical bands, so even single-epoch NIR observations are sufficient to approximate the mean magnitudes. Moreover, Soszyński et al. (2005) showed that phase offsets and amplitude ratios between NIR and visual light curves

[1]Based on observations obtained with the ESO VLT for Large Programme 171.D-0004

of the fundamental mode Cepheids are very stable. Thus, it is possible to accurately transform random-phase single-epoch JHK observations to mean magnitudes using the complete optical light curves.

Studying simultaneously the NIR and optical PL relations of Cepheids provides one additional advantage. It allows to precisely determine the total reddening, and measure the distance to nearby galaxies with an unprecedented accuracy of better than 3% (Gieren et al. 2005a, 2006; Pietrzyński et al. 2006a).

NGC 3109 is a well-studied galaxy on the periphery of the Local Group. It has been classified as an irregular galaxy (Irr; Sandage 1961), a dwarf spiral (Sm; Sandage & Tammann 1981) or a dwarf barred spiral (SBm; de Vaucouleurs et al. 1991). The galaxy is seen almost edge-on at an inclination of $75^\circ \pm 2$ and a position angle of the disk of $93^\circ \pm 2$ (Jobin & Carignan 1990). The mean metallicity of the old stellar population was estimated to be about -1.7 dex (Méndez et al. 2002). Little is known about the metallicity of the young stellar population of NGC 3109. For one H II region in this galaxy Lee et al. (2003) have determined an oxygen abundance of about -1.0 dex, which should be representative for the average metallicity of the Cepheids.

NGC 3109 is one of the largest and brightest Local Group galaxies visible in the Southern hemisphere, and as such it was added to the list of targets observed in the course of the Araucaria Project (Gieren et al. 2005b). The project aims at determining accurate distances to a number of nearby galaxies and investigating the environmental dependences of a number of stellar indicators: Cepheids, RR Lyrae stars, blue supergiants, the tip of the red giant branch and red clump stars.

Historically, the first attempt of a Cepheid distance determination to NGC 3109 was made by Demers et al. (1985), who used photographic observations to discover 5 Cepheids in this galaxy. They obtained a true distance modulus of $(m - M)_0 = 25.98 \pm 0.15$ mag. This value, and all other distance estimations presented in this paper, is tied to an assumed Large Magellanic Cloud (LMC) distance modulus of 18.50 mag. Sandage & Carlson (1988) increased the number of known Cepheids in NGC 3109 to 29, and suggested the same distance modulus to NGC 3109. Subsequent CCD photometry (Capaccioli et al. 1992) revealed systematic errors in the previous photographic data, and adjusted the distance modulus estimation to $(m - M)_0 = 25.5 \pm 0.2$ mag. This revision corresponded to a distance about 25% shorter than the one obtained by Demers et al. (1985) and Sandage & Carlson (1988). Musella et al. (1997) increased the number of known Cepheids in NGC 3109 by another 16 objects and secured multiwavelength ($BVRI$) photometry for some of them. They obtained a true distance modulus of $(m-M)_0 = 25.67 \pm 0.16$ mag, but they adopted a total interstellar reddening $E(B-V) = 0$, because their forced solution yielded a negative reddening value.

Recently, Pietrzyński et al. (2006b, hereafter Paper I) presented a catalog of 113 Cepheids in NGC 3109 discovered from V and I observations collected with the 1.3-m Warsaw Telescope at Las Campanas Observatory. 76 of these objects were not known before, and for the remaining 37 Cepheids improved periods were measured. Adopting a total reddening $E(B-V) = 0.1$ mag a true distance modulus $(m-M)_0 = 25.54 \pm 0.05$ mag (statistical error) was obtained.

In this work, we extend the light curve coverage for 77 of the Cepheids presented in Paper I to the NIR J and K bands. We utilize multiband NIR/optical photometry for an accurate determination of the distance, and the total (average) interstellar extinction to the Cepheids in NGC 3109.

The paper is composed as follows. In Section 2, we describe the J and K band observations, data reductions and calibration of the photometry. In Sections 3 and 4, we derive the Cepheid PL relations from our data and determine the true distance modulus to NGC 3109 with the mean color excess. Our results are discussed and summarized in Sections 5 and 6.

2. Observations and Data Reduction

We used deep J- and K-band images recorded with the 8.2-m ESO Very Large Telescope equipped with the Infrared Spectrometer And Array Camera (ISAAC). Fig. 1 shows the location of the three $2\farcm5 \times 2\farcm5$ fields observed in service mode on 6 nights between 31 Jan and 19 Feb 2004. Each field was observed in J and K bands two times on two different nights, with exception of the field F-I, for which data in the J band was only obtained once. Observations were carried out using a jitter imaging technique, with a dithering of the frames following a random pattern characterized by typical offsets about $10''$. The final frames in the J and K bands were obtained as a co-addition of 32 and 88 single exposures obtained with integration times 30 s and 15 s, respectively. Thus, the total exposure time for a given observation was 16 minutes in J and 22 minutes in K. The observations were obtained under very good seeing conditions. During four of six observing nights photometric standard stars on the UKIRT system (Hawarden et al. 2001) were observed along with the science fields.

The images were reduced using the program JITTER from the ECLIPSE package developed by ESO to reduce the NIR data. The PSF photometry was obtained with the programs DAOPHOT and ALLSTAR. The PSF model was derived iteratively from 20-30 isolated bright stars following the procedure described by Pietrzyński et al. (2002). In order to convert our profile photometry to the aperture system, aperture corrections were computed using the same stars as for the calculation of the PSF model. The median of the aperture corrections

obtained for all the stars was finally adopted as the aperture correction for a given frame. The aperture photometry for our standard stars was performed with DAOPHOT using the same aperture as for the calculation of the aperture corrections. The photometry obtained on the two nights with no standard observations was tied to the standard system using several hundred comparison stars.

The astrometric solution for the observed fields was performed by cross-identification of the brightest stars in each field with the Infrared Digitized Sky Survey 2 (DSS2-infrared) images. We used programs developed by Udalski et al. (1998) to calculate the transformations between pixel grid of our images and equatorial coordinates of the DSS astrometric system. The internal error of the transformation is less than 0.3 arcsec, but systematic errors of the DSS coordinates can be up to about 0.7 arcsec.

We performed an external check of our photometry by comparing the magnitudes of the brightest stars ($K < 16$ mag, $J < 17$ mag) with the 2MASS Point Source Catalog (Cutri et al. 2003). Unfortunately, even the most luminous stars in our dataset are close to the limiting magnitudes of the 2MASS catalog. Only about one dozen 2MASS stars identified with our objects have photometric errors smaller than 0.1 mag. However, for these stars we have not noticed any evident zero point offsets between both datasets. We estimate that the agreement between the zero points of both photometries is better than 0.03 mag.

Our three fields in the central regions of NGC 3109 contain 77 of the 113 Cepheids listed in Paper I. All the individual observations in K and J are given in Table 1, which lists the stars' IDs, Heliocentric Julian Day of the observations, and measurements in K and J with the standard deviations. For most of the stars we collected two observations per given filter. The exception are J-band observations of stars in the field F-I for which only one point was secured. There are some other objects for which we obtained only one observation in the J or K band. For most of these cases the cause was the location of the variable close to the edge of the field and imperfections of the telescope pointing. On the other hand, there are three variables for which we collected more than two data points because they were located in the overlapping parts of adjacent fields.

3. The Cepheid Period–Luminosity Relations in J and K

All the individual J and K measurements reported in Table 1 were transformed to the mean magnitudes of the Cepheids using the recipe given by Soszyński et al. (2005). The corrections were derived using the complete V-band light curves from Paper I. For the vast majority of our Cepheids the mean magnitudes obtained from the independent

measurements at different phases agreed very well, especially for objects discovered during the earlier surveys (Sandage & Carlson 1988; Musella et al. 1997) for which improved periods were available. The precisely determined V-band phases are of crucial importance for the accuracy of the estimated mean K and J magnitudes. For most of our objects, the difference between the two estimates of the mean magnitude were comparable with the measurement errors of the original points.

Table 2 gives the intensity mean J and K magnitudes of our sample of Cepheids. Each value was derived as an average from the individual determinations of the mean luminosities. In Table 2, we also provide the periods (from Paper I), uncertainties on the mean magnitudes (which contain the intrinsic error 0.03 mag of the mean magnitude estimation technique) and remarks on some of the variables.

In Fig. 2, we display the J- and K-band PL diagrams for the Cepheids in NGC 3109. Following Paper I, the Cepheids with $\log P < 0.75$ were excluded from our distance determination. In this range of periods the scatter of points around the average PL relation substantially grows, which is an effect of the larger photometric errors and the contamination with probable first overtone pulsators. It is also clearly appreciated from Fig. 2 that below our adopted cutoff period a Malmquist bias begins to appear, due to the depth limit of our photometry. Especially in the K band, for smaller periods we see only the Cepheids lying towards the bright end of the instability strip at these periods, whereas the fainter Cepheids are mostly below the detection threshold.

Ideally, we should retain the same value of the cutoff period for all our target galaxies. However, in practice this is not the best solution because our photometry extends to different levels of faintness in the different galaxies our program, corresponding to different periods at which an incompleteness bias begins to be a serious problem. Also, there is quite a variety in the relative numbers of long- and short-period Cepheids in the different galaxies, making the choice of a uniform value of the cutoff period difficult. We can, however, check on the effect of changing the cutoff period to larger values. Our present solution for the distance modulus of NGC 3109 (see below) changes by less than 0.01 mag if the cutoff period of $\log P = 0.75$ is changed to values of 0.80, 0.90, and 1.0. In the J band, the maximum change is 0.04 mag, or 2%, which is 1 σ, and therefore not significant. We therefore conclude that our distance result for NGC 3109 does not depend in any significant way on the adopted cutoff period (as long as its value is large enough to avoid the problem of Malmquist bias and contamination with overtone Cepheids).

We also omitted 5 variables with periods longer than our adopted cutoff period, but significantly brighter than the ridge line luminosity at the respective periods. All these outliers from the NIR PL relation are also overluminous in the V and I bands (Paper I),

though, in some cases, the NIR deviation is larger than in the visual bands. A possible explanation of this behavior is the presence of a bright red companion star (but see our discussion). All the excluded objects are marked with empty circles in Fig. 2.

The straight lines superimposed in Fig. 2 are the best-fitting linear functions with slopes adopted from the LMC Cepheids as given by Persson et al. (2004): -3.153 ± 0.051 and -3.261 ± 0.042 for J and K bands, respectively. Free least-square fits to the PL relations yield somewhat shallower slopes: -2.85 ± 0.12 for J and -3.11 ± 0.12 for the K-band, but still statistically consistent with the Persson et al. slopes. The weighted least-squares fits with forced slopes yield the following relations:

$$J = -3.153 \log P + 23.452(\pm 0.028), \quad \sigma = 0.178$$
$$K = -3.261 \log P + 23.123(\pm 0.027), \quad \sigma = 0.181$$

To determine the relative distance moduli between NGC 3109 and LMC we need to convert the NICMOS (LCO) photometric system used by Persson et al. (2004) to the UKIRT system utilized in this paper. According to Hawarden et al. (2001), the magnitudes in both systems differ by constant, color-independent values: 0.034 ± 0.004 and 0.015 ± 0.007 for the J and K wavebands, respectively. Applying these offsets, we obtained the following relative apparent distance moduli with respect to the LMC: $\delta(m-M)_J = 7.150 \pm 0.028$ mag and $\delta(m-M)_K = 7.102 \pm 0.027$ mag, or, assuming the LMC distance modulus of 18.5 mag, $(m-M)_J = 25.650 \pm 0.028$ mag and $(m-M)_K = 25.602 \pm 0.027$ mag.

Taking into consideration the apparent distance moduli measured in the V and I bands in Paper I, $(m-M)_V = 25.854 \pm 0.027$ mag and $(m-M)_I = 25.739 \pm 0.026$ mag, we can determine the true distance modulus and total interstellar reddening to NGC 3109. In Fig. 3 we present the apparent distance moduli for the V, I, J and K wavebands plotted against the total-to-selective absorption provided by the Schlegel et al. (1998) reddening law. One can notice the extraordinary agreement between the measured distance moduli and the linear function fitted to the points. The slope and the intersection of this relation give $E(B-V)$ and the true distance modulus to the galaxy, respectively. The best-fitting relation yields:

$$E(B-V) = 0.087 \pm 0.012 \text{ mag}$$
$$(m-M)_0 = 25.571 \pm 0.024 \text{ mag}$$

corresponding to a distance 1.30 Mpc $\pm$ 0.02 Mpc.

4. Period – NIR Wesenheit Index Relation

The Wesenheit index (Madore 1982) is a reddening-free quantity defined as a linear combination of the selected magnitude and color of the star. For example, for J and K magnitudes it is defined as:

$$W_{JK} = K - \frac{A_K}{E(J-K)}(J-K)$$

Using Schlegel's et al. (1998) ratios of total-to-selective absorption measured for the UKIRT system ($R_J = 0.902$, $R_K = 0.367$), we obtain $A_K/E(J-K) = 0.686$. The advantage of using the Wesenheit index is the canceling of the interstellar extinction effect star by star without explicitly determining this effect.

Fig. 4 shows the period–W_{JK} diagram for our sample of Cepheids in NGC 3109. The straight line shows the linear least-squares fit to the selected Cepheids indicated with filled circles. Similarly to the procedure adopted for the J and K bands, we force the slope of the $\log P$–W_{JK} relation to the relation defined by the LMC Cepheids (Persson et al. 2004). After converting Persson's et al. photometry onto the UKIRT system, we obtained the following period–W_{JK} relation for the LMC Cepheids:

$$W_{JK} = -3.374 \log P + 15.865$$

Solving for the best coefficients of the period–W_{JK} relation in NGC 3109 leads to the following relation:

$$W_{JK} = -3.374 \log P + 22.944(\pm 0.030)$$

which corresponds to a NGC 3109 distance modulus of 25.579 mag. This value is fully consistent with the true distance modulus obtained from the multiwavelength analysis.

5. Discussion

An exhaustive discussion about possible systematic errors that can affect our distance determination was presented by Gieren et al. (2005a, 2006) and Pietrzyński et al. (2006a). Here we describe only the most important issues concerning this subject.

The source of largest systematic error on our distance determination is probably the unsolved problem of the LMC distance modulus. The possible uncertainty on the distance to the LMC may exceed 10%. For consistency with our previous work, as well as with many other extragalactic distance determinations, we assumed that the true distance modulus to the LMC is equal to 18.50 mag. If future studies change this determination our distance moduli can be easily transformed to the proper value.

Another potential source of systematic uncertainty of our results is the unknown effect of metal abundances on the slopes and zero points of Cepheid *PL* relations. To date very few empirical studies deal with this problem, especially in the NIR domain. Theoretical considerations are also inconclusive. Linear pulsation models (e.g. Saio & Gautschy 1998; Sandage et al. 1999; Alibert et al. 1999; Baraffe & Alibert 2001) suggest that the dependence of the Cepheid *PL* relation on chemical composition is very weak. On the other hand, the nonlinear models (e.g. Bono et al. 1999; Caputo et al. 2000) predict that metal-rich Cepheids are significantly fainter than metal-poor ones, but the effect decreases with increasing wavelength. In our previous studies (Gieren et al. 2005a, 2006; Pietrzyński et al. 2006a) we have not noticed any statistically significant relationships between slopes of the NIR *PL* relations and mean metallicities. In the case of NGC 3109 the *PL* relation seem somewhat shallower than in the LMC, but taking into account the relatively smaller range of periods, the disagreement is statistically insignificant. Our knowledge about the influence of metallicity on the zero points of the NIR *PL* relations is even more incomplete. While preliminary results from our project seem to indicate that the effect of metallicity on the *PL* relation zero point is very modest (Pietrzyński & Gieren 2002), we will have a much better database to investigate the effect once we have measured the distances to all our target galaxies with a variety of methods, including red clump stars (Pietrzyński et al. 2003), and the blue supergiant Flux-Weighted Gravity-Luminosity Relation (Kudritzki et al. 2003). We will therefore leave an exhaustive discussion of this point to a later stage of the Araucaria Project, and for the time being *assume* that the Cepheid *PL* relation is universal.

Selection effects, such as an inhomogeneous distribution of the Cepheids in the instability strip, do not influence significantly the total error because our Cepheid sample is large enough to minimize such random effects. Our variables seem to be randomly distributed across the strip, with no tendency for grouping near the red or blue edges.

Similar conclusions can be drawn for possible crowding effects. Recently, Bresolin et al. (2005) demonstrated that blending in the Sculptor galaxy NGC 300 affects the distance determination from ground-based Cepheid photometry by less than 2%. In the case of NGC 3109, the effect should be even smaller because the galaxy is much closer, and the average density of stars is smaller.

The group of five overluminous stars in the period–luminosity diagrams which were excluded in the distance determination are potentially interesting objects. While one possibility for their excessive brightness is that they are normal Cepheids which are blended with very bright unresolved stars, it is intriguing that *all* these objects are about 1 mag brighter than the PL relation at the corresponding period. If blending was the cause for the over-brightness of these stars, one might expect a continuum of luminosity offsets, and not the same value for each of them. This might suggest that an *intrinsic* cause is responsible for these objects to be so luminous. If these objects are binary Cepheids, they would certainly harbour some very interesting new information on binary star formation for massive stars. Such an investigation is beyond the scope of this work, however. We just mention that very similar, overluminous Cepheids are also seen in IC 1613 (Pietrzyński et al. 2006a), and NGC 6822 (Gieren et al. 2006), making it worthwhile to look more closely into the nature of these stars.

From this discussion, and from the conclusions presented in the previous papers of this series we conclude that the total systematic error on our distance determination does not exceed ∼3%. However, one should remember that this estimate does not contain the currently largest uncertainty – the still debated distance modulus to the LMC.

Our determination of the total color excess ($E(B-V) = 0.087$ mag), based on the multiwavelength approach, can be compared with the Galactic reddening maps of Schlegel et al. (1998). According to these maps, the foreground $E(B-V)$ changes across NGC 3109 from 0.03 to 0.07 mag. Our estimation then indicates that the *intrinsic* average reddening in NGC 3109 appropriate to the Cepheids is about 0.04 mag.

6. Summary and Conclusions

All previous CCD surveys for Cepheids in NGC 3109 were carried out at blue wavelengths, thus the effect of obscuration by interstellar dust was a significant factor affecting the final results. In the present study, we present for the first time NIR CCD photometry of the Cepheids in this galaxy, and we have determined an accurate distance and reddening. Although NGC 3109 does not contain a population of very long-period Cepheids, which carry the strongest weight in the distance determinations, we were able to measure the distance to this galaxy relative to the LMC with an accuracy of about 3%.

In Table 3, we list the most important previous distance determinations to NGC 3109. Fig. 5 shows the same results in a different way, highlighting the trend of increasing accuracy in the results over the past two decades. It can be appreciated that our result derived in

this paper is in excellent agreement with the most recent estimations of the distance to NGC 3109, but it is clearly more accurate and will therefore be very useful for an improved determination of environmental effects on stellar distance indicators. Such studies will be the subject of forthcoming papers which will take advantage of the series of accurate Cepheid distances to nearby galaxies from NIR photometry which we are providing in our project.

WG and GP gratefully acknowledge financial support for this work from the Chilean Center for Astrophysics FONDAP 15010001. Support from the Polish KBN grant No 2P03D02123 and BST grant to Warsaw University Observatory is also acknowledged. We thank the ESO OPC for the generous amounts of observing time at Paranal and La Silla telescopes allocated to our Large Programme. Special thanks goes to the Paranal staff astronomers for their expert help in obtaining the high-quality data which form the basis for the work reported in this paper.

REFERENCES

Alibert, Y., Baraffe, I., Hauschildt, P., & Allard, F. 1999, A&A, 344, 551

Baraffe, I., & Alibert, Y. 2001, A&A, 371, 592

Bono, G., Caputo, F., Castellani, V., & Marconi, M. 1999, ApJ, 512, 711

Bresolin, F., Pietrzyński, G., Gieren, W., & Kudritzki, R.-P. 2005, ApJ, 634, 1020

Capaccioli, M., Piotto, G., & Bresolin, F. 1992, AJ, 103, 1151

Caputo, F., Marconi, M., & Musella, I. 2000, A&A, 354, 610

Cutri, R. M. et al. 2003, 2MASS All-Sky Catalog of Point Sources

Demers, S., Irwin, M. J., & Kunkel, W. E. 1985, AJ, 90, 1967

de Vaucouleurs, G., de Vaucouleurs, A., Corwin, H. G., Buta, R. J., Paturel, G., & Fouque, P. 1991, Third Reference Catalogue of Bright Galaxies (New York: Springer)

Elias, J. H., & Frogel, J. A. 1985, ApJ, 289, 141

Gieren, W., Pietrzyński, G., Soszyński, I., Bresolin, F., Kudritzki, R.-P., Minniti, D., & Storm, J. 2005a, ApJ, 628, 695

Gieren, W., Pietrzyński, G., Bresolin, F., Kudritzki, R.-P., Minniti, D., Urbaneja, M., Soszyński, I., Storm, J., Fouque, P., Bono, G., Walker, A. & Garcia, J. 2005b, The Messenger, 121, 23

Gieren, W., Pietrzyński, G., Nalewajko, K., Soszyński, I., Bresolin, F., Kudritzki, R.-P., Minniti, D., & Romanowsky, A. 2006, ApJ, in press (astro-ph/0605231)

Hawarden, T. G., Leggett, S. K., Letawsky, M. B., Ballantyne, D. R., & Casali, M. M. 2001, MNRAS, 325, 563

Jobin, M., & Carignan, C. 1990, AJ, 100, 648

Karachentsev, I. D., Sharina, M. E., Makarov, D. I., et al. 2002, A&A, 389, 812

Kudritzki, R. P., Bresolin, F., & Przybilla, N. 2003, ApJ, 582, L83

Lee, M. G. 1993, ApJ, 408, 409

Lee, H., Grebel, E. K., & Hodge, P. W. 2003, A&A, 401, 141

Madore, B. F. 1982, ApJ, 253, 575

Madore, B. F., & Freedman, W. L. 1991, PASP, 103, 933

McGonegal, R., McAlary, C. W., Madore, B. F., & McLaren, R. A. 1982, ApJ, 257, L33

Méndez, B., Davis, M., Moustakas, J., Newman, J., Madore, B. F., & Freedman, W. L. 2002, AJ, 124, 213

Minniti, D., Zijlstra, A. A., & Alonso, M. V. 1999, AJ, 117, 881

Musella, I., Piotto, G., & Capaccioli, M. 1997, AJ, 114, 976

Persson, S. E., Madore, B. F., Krzemiński, W., Freedman, W. L., Roth, M., & Murphy, D. C. 2004, AJ, 128, 2239

Pietrzyński, G., & Gieren, W. 2002, AJ, 124, 2633

Pietrzyński, G., Gieren, W., & Udalski, A. 2002, PASP, 114, 298

Pietrzyński, G., Gieren, W., & Udalski, A. 2003, AJ, 125, 2494

Pietrzyński, G., Gieren, W., Soszyński, I., Bresolin, F., Kudritzki, R.-P., Dall'Ora M., Storm, J., & Bono, B. 2006a, ApJ, 642, 216

Pietrzyński, G., Gieren, W., Udalski, A., Soszyński, I., Bresolin, F., Kudritzki, R.-P., Mennickent R., Kubiak, M., Szymański, M., & Hidalgo, S. 2006b, ApJ, in press (astro-ph/0605226; Paper I)

Richer, M. G., & McCall, M. L. 1992, AJ, 103, 54

Saio, H., & Gautschy, A. 1998, ApJ, 498, 360

Sandage, A. 1961, The Hubble Atlas of Galaxies (Carnegie Inst. of Washington)

Sandage, A., & Tammann, G. A. 1981, A revised Shapley-Ames Catalog of bright galaxies (Carnegie Inst. of Washington)

Sandage, A., & Carlson, G. 1988, AJ, 96, 1599

Sandage, A., Bell, R. A., & Tripicco, M. J. 1999, ApJ, 522, 250

Schlegel, D. J., Finkbeiner, D. P., & Davis, M. 1998, ApJ, 500, 525

Soszyński, I., Gieren, W., & Pietrzyński, G. 2005, PASP, 117, 823

Udalski, A., Szymański, M., Kubiak, M., Pietrzyński, G., Woźniak, P., & Żebruń, K. 1998, Acta Astron., 48, 147

Table 1. Journal of the individual J and K observations of the NGC 3109 Cepheids.

ID	J HJD	J	σ_J	K HJD	K	σ_K
cep001	–	–	–	2453036.80998	18.392	0.020
cep001	2453047.68199	18.730	0.014	2453047.76282	18.265	0.018
cep002	2453037.69282	18.966	0.021	2453037.76573	18.374	0.025
cep002	2453049.67836	18.730	0.041	2453049.74253	18.165	0.016
cep003	–	–	–	2453036.80998	18.632	0.026
cep003	2453047.68199	19.017	0.024	2453047.76282	18.495	0.026
cep004	–	–	–	2453036.80998	18.643	0.023
cep004	2453047.68199	18.882	0.014	2453047.76282	18.394	0.019
cep005	2453037.69282	19.338	0.030	2453037.76573	18.831	0.039
cep005	2453049.67836	18.899	0.030	2453049.74253	18.352	0.027
cep007	2453045.77048	19.873	0.023	2453045.83694	19.255	0.035
cep007	2453055.62418	19.715	0.031	2453055.70117	19.237	0.029
cep009	2453045.77048	19.408	0.022	2453045.83694	18.829	0.024
cep009	2453055.62418	19.231	0.032	2453055.70117	18.865	0.021
cep011	2453045.77048	19.874	0.026	2453045.83694	19.342	0.037
cep011	2453055.62418	19.649	0.032	2453055.70117	19.121	0.027
cep012	2453045.77048	19.739	0.029	2453045.83694	19.286	0.048
cep012	2453055.62418	19.938	0.048	2453055.70117	19.338	0.039
cep014	2453037.69282	19.616	0.041	2453037.76573	19.236	0.042
cep014	2453045.77048	19.486	0.026	2453045.83694	19.202	0.036
cep014	2453049.67836	19.777	0.057	2453049.74253	19.221	0.035
cep014	2453055.62418	19.764	0.051	2453055.70117	19.448	0.032
cep015	–	–	–	2453036.80998	19.250	0.036
cep015	2453047.68199	19.847	0.027	2453047.76282	19.334	0.032
cep016	2453037.69282	19.540	0.025	2453037.76573	19.315	0.038
cep016	2453049.67836	19.800	0.039	2453049.74253	19.291	0.024
cep017	2453045.77048	19.789	0.024	2453045.83694	19.353	0.035
cep017	2453055.62418	20.061	0.039	2453055.70117	19.590	0.032
cep018	2453037.69282	20.078	0.043	2453037.76573	19.597	0.041
cep018	2453049.67836	20.076	0.072	–	–	–
cep020	2453045.77048	20.250	0.029	2453045.83694	19.852	0.048

Table 1—Continued

ID	J HJD	J	σ_J	K HJD	K	σ_K
cep020	2453055.62418	20.250	0.036	2453055.70117	19.639	0.033
cep022	2453045.77048	19.907	0.038	2453045.83694	19.501	0.052
cep022	2453055.62418	19.775	0.057	2453055.70117	19.479	0.037
cep023	2453045.77048	19.625	0.021	2453045.83694	19.032	0.029
cep023	2453055.62418	19.553	0.044	2453055.70117	19.142	0.025
cep025	2453045.77048	18.638	0.018	2453045.83694	17.826	0.016
cep025	2453055.62418	18.695	0.027	2453055.70117	17.803	0.019
cep026	2453037.69282	20.298	0.045	2453037.76573	19.874	0.053
cep027	2453045.77048	20.125	0.029	2453045.83694	19.634	0.058
cep027	2453055.62418	20.188	0.052	2453055.70117	19.776	0.035
cep028	–	–	–	2453036.80998	19.561	0.036
cep028	2453047.68199	20.206	0.038	2453047.76282	19.688	0.051
cep029	2453037.69282	19.880	0.035	2453037.76573	19.388	0.042
cep029	2453049.67836	19.818	0.042	2453049.74253	19.276	0.024
cep030	2453037.69282	20.397	0.048	2453037.76573	20.043	0.044
cep030	2453049.67836	20.321	0.081	2453049.74253	19.789	0.037
cep031	2453045.77048	19.934	0.028	2453045.83694	19.452	0.044
cep031	2453055.62418	20.020	0.035	2453055.70117	19.463	0.030
cep032	2453037.69282	20.479	0.043	2453037.76573	19.666	0.062
cep032	2453049.67836	20.351	0.055	2453049.74253	19.529	0.059
cep035	2453047.68199	20.043	0.050	2453047.76282	19.720	0.059
cep036	2453037.69282	20.182	0.053	2453037.76573	19.811	0.049
cep036	2453049.67836	20.266	0.076	2453049.74253	19.997	0.043
cep038	–	–	–	2453036.80998	19.990	0.043
cep038	2453047.68199	20.392	0.044	2453047.76282	19.926	0.054
cep039	2453045.77048	20.609	0.047	2453045.83694	20.229	0.067
cep039	2453055.62418	20.515	0.068	2453055.70117	20.201	0.043
cep043	–	–	–	2453036.80998	20.105	0.058
cep043	2453047.68199	20.409	0.042	2453047.76282	20.392	0.084
cep047	–	–	–	2453036.80998	19.737	0.043
cep047	2453047.68199	20.401	0.048	2453047.76282	19.948	0.066

Table 1—Continued

ID	J HJD	J	σ_J	K HJD	K	σ_K
cep048	2453037.69282	20.586	0.038	2453037.76573	20.256	0.059
cep048	2453049.67836	20.468	0.073	2453049.74253	19.722	0.033
cep050	–	–	–	2453036.80998	19.955	0.042
cep050	2453047.68199	20.707	0.064	2453047.76282	20.305	0.068
cep051	2453045.77048	20.549	0.038	2453045.83694	20.518	0.076
cep051	2453055.62418	20.462	0.055	2453055.70117	20.054	0.042
cep052	–	–	–	2453036.80998	20.153	0.055
cep052	2453047.68199	20.530	0.049	2453047.76282	20.215	0.058
cep053	–	–	–	2453036.80998	20.020	0.048
cep053	2453047.68199	20.816	0.054	2453047.76282	20.532	0.086
cep054	–	–	–	2453036.80998	20.002	0.047
cep054	2453047.68199	20.533	0.044	2453047.76282	20.340	0.072
cep055	–	–	–	2453036.80998	19.929	0.061
cep055	2453047.68199	20.695	0.059	2453047.76282	20.199	0.064
cep056	2453045.77048	19.782	0.037	2453045.83694	18.693	0.027
cep056	2453055.62418	20.012	0.039	2453055.70117	18.735	0.048
cep057	2453037.69282	19.957	0.038	2453037.76573	19.021	0.067
cep057	2453049.67836	19.571	0.051	2453049.74253	18.810	0.069
cep058	2453045.77048	20.839	0.049	2453045.83694	20.521	0.092
cep058	2453055.62418	20.608	0.059	2453055.70117	20.522	0.068
cep059	2453045.77048	20.901	0.043	2453045.83694	20.475	0.083
cep059	2453055.62418	20.644	0.063	2453055.70117	20.210	0.039
cep060	–	–	–	2453036.80998	20.225	0.048
cep060	2453047.68199	20.927	0.059	2453047.76282	20.494	0.074
cep061	–	–	–	2453036.80998	19.392	0.073
cep061	2453047.68199	19.683	0.041	2453047.76282	19.241	0.047
cep063	2453045.77048	20.395	0.049	2453045.83694	20.252	0.133
cep064	2453037.69282	20.832	0.039	2453037.76573	20.255	0.057
cep064	2453049.67836	20.594	0.075	–	–	–
cep066	2453037.69282	20.800	0.046	2453037.76573	20.152	0.070
cep066	2453045.77048	20.513	0.062	2453045.83694	20.028	0.072

Table 1—Continued

ID	J HJD	J	σ_J	K HJD	K	σ_K
cep066	2453049.67836	20.576	0.136	2453049.74253	20.658	0.044
cep066	2453055.62418	20.603	0.073	2453055.70117	20.376	0.055
cep067	2453037.69282	21.140	0.043	2453037.76573	20.601	0.065
cep067	2453049.67836	20.973	0.160	2453049.74253	20.604	0.048
cep067	2453055.62418	21.029	0.083	2453055.70117	20.616	0.077
cep068	2453037.69282	20.498	0.034	2453037.76573	20.120	0.053
cep068	2453049.67836	20.665	0.105	2453049.74253	20.538	0.042
cep069	2453045.77048	19.927	0.029	2453045.83694	19.158	0.033
cep069	2453055.62418	20.084	0.038	2453055.70117	19.222	0.036
cep072	2453045.77048	20.475	0.039	2453045.83694	20.140	0.068
cep072	2453055.62418	20.980	0.065	2453055.70117	20.381	0.063
cep073	2453045.77048	20.647	0.045	2453045.83694	20.206	0.063
cep073	2453055.62418	20.891	0.078	2453055.70117	20.554	0.049
cep074	2453037.69282	20.781	0.053	2453037.76573	20.499	0.083
cep074	2453049.67836	20.818	0.096	2453049.74253	20.421	0.062
cep075	2453037.69282	21.113	0.052	2453037.76573	20.732	0.082
cep075	2453049.67836	21.136	0.114	2453049.74253	20.663	0.057
cep076	–	–	–	2453036.80998	20.381	0.062
cep076	2453047.68199	20.820	0.061	2453047.76282	20.581	0.081
cep077	2453037.69282	21.029	0.050	2453037.76573	20.431	0.076
cep077	2453049.67836	21.142	0.118	2453049.74253	20.484	0.080
cep078	2453045.77048	21.156	0.092	2453045.83694	20.947	0.164
cep078	2453055.62418	21.153	0.084	2453055.70117	20.692	0.066
cep079	2453037.69282	21.279	0.069	2453037.76573	20.423	0.080
cep079	2453049.67836	20.727	0.162	2453049.74253	20.685	0.047
cep080	2453045.77048	20.688	0.054	2453045.83694	20.466	0.082
cep080	2453055.62418	20.945	0.096	2453055.70117	20.592	0.074
cep084	2453047.68199	20.877	0.085	2453047.76282	20.569	0.118
cep088	2453037.69282	19.652	0.027	2453037.76573	18.678	0.024
cep088	2453049.67836	19.633	0.030	2453049.74253	18.606	0.023
cep090	2453037.69282	20.940	0.051	2453037.76573	20.441	0.073

Table 1—Continued

ID	J HJD	J	σ_J	K HJD	K	σ_K
cep090	2453049.67836	21.047	0.094	2453049.74253	20.390	0.058
cep092	2453045.77048	21.017	0.043	2453045.83694	20.572	0.087
cep092	2453055.62418	21.314	0.066	2453055.70117	20.473	0.072
cep094	2453037.69282	21.130	0.041	2453037.76573	20.576	0.076
cep094	2453049.67836	21.284	0.138	2453049.74253	20.895	0.060
cep095	–	–	–	2453036.80998	19.765	0.051
cep095	2453047.68199	20.420	0.050	2453047.76282	19.702	0.061
cep096	–	–	–	2453036.80998	20.633	0.077
cep096	2453047.68199	20.476	0.055	–	–	–
cep097	2453045.77048	21.048	0.052	2453045.83694	20.725	0.098
cep097	2453055.62418	20.892	0.066	2453055.70117	20.413	0.054
cep098	–	–	–	2453036.80998	19.728	0.045
cep098	2453047.68199	20.296	0.038	2453047.76282	19.874	0.052
cep099	2453045.77048	21.000	0.061	2453045.83694	20.377	0.080
cep099	2453055.62418	20.915	0.094	2453055.70117	20.785	0.058
cep100	2453045.77048	21.580	0.084	2453045.83694	20.691	0.105
cep100	2453055.62418	21.695	0.092	2453055.70117	20.969	0.098
cep101	2453037.69282	21.250	0.072	2453037.76573	20.610	0.094
cep103	2453045.77048	21.235	0.066	2453045.83694	20.801	0.108
cep103	2453055.62418	21.015	0.104	2453055.70117	21.059	0.064
cep104	–	–	–	2453045.83694	19.336	0.039
cep104	2453055.62418	20.661	0.042	2453055.70117	19.187	0.265
cep105	–	–	–	2453036.80998	20.525	0.089
cep105	2453047.68199	20.682	0.067	–	–	–
cep108	2453045.77048	21.395	0.063	–	–	–
cep108	2453055.62418	21.586	0.122	2453055.70117	21.143	0.082
cep110	–	–	–	2453036.80998	20.590	0.085
cep110	2453047.68199	20.874	0.063	2453047.76282	20.334	0.084

Table 2. Intensity mean J and K magnitudes for 77 Cepheids in NGC 3109

ID	P	$\langle J \rangle$	$\sigma_{\langle J \rangle}$	$\langle K \rangle$	$\sigma_{\langle K \rangle}$	Remarks
cep001	31.4793	18.864	0.033	18.413	0.028	
cep002	31.270	18.825	0.039	18.242	0.030	
cep003	29.110	19.077	0.038	18.544	0.034	
cep004	27.389	18.950	0.033	18.502	0.030	
cep005	26.8274	19.068	0.037	18.551	0.040	
cep007	20.388	19.795	0.035	19.252	0.039	
cep009	19.5759	19.328	0.035	18.861	0.031	
cep011	17.2293	19.767	0.036	19.261	0.039	
cep012	14.750	19.812	0.045	19.265	0.049	
cep014	14.062	19.650	0.048	19.282	0.039	
cep015	14.030	19.949	0.040	19.375	0.040	
cep016	13.9047	19.648	0.039	19.229	0.038	
cep017	13.6250	19.890	0.039	19.418	0.040	
cep018	13.364	20.189	0.063	19.675	0.051	
cep020	13.011	20.230	0.039	19.757	0.046	
cep022	11.864	19.836	0.053	19.520	0.050	
cep023	11.707	19.660	0.040	19.166	0.034	
cep025	11.596	18.600	0.031	17.769	0.028	blend?
cep026	11.534	20.423	0.054	19.949	0.061	
cep027	11.238	20.108	0.047	19.641	0.052	
cep028	11.0663	20.295	0.048	19.715	0.049	
cep029	10.903	19.798	0.044	19.306	0.040	
cep030	10.887	20.198	0.070	19.799	0.046	
cep031	10.851	20.025	0.038	19.492	0.043	
cep032	10.826	20.316	0.054	19.520	0.064	
cep035	9.7501	20.071	0.058	19.773	0.066	
cep036	9.4084	20.270	0.069	19.957	0.051	
cep038	9.3242	20.408	0.053	20.011	0.053	
cep039	9.11136	20.608	0.062	20.291	0.060	
cep043	8.7970	20.306	0.052	20.215	0.075	
cep047	8.55708	20.262	0.057	19.833	0.060	

Table 2—Continued

ID	P	$\langle J \rangle$	$\sigma_{\langle J \rangle}$	$\langle K \rangle$	$\sigma_{\langle K \rangle}$	Remarks
cep048	8.4791	20.530	0.062	19.980	0.052	
cep050	8.24330	20.592	0.071	20.149	0.060	
cep051	8.19173	20.597	0.052	20.352	0.065	
cep052	8.10451	20.541	0.057	20.251	0.060	
cep053	7.9351	20.651	0.062	20.301	0.073	
cep054	7.9038	20.456	0.053	20.131	0.064	
cep055	7.7960	20.706	0.066	20.105	0.066	
cep056	7.77376	19.853	0.044	18.717	0.044	blend?
cep057	7.5389	19.834	0.050	18.952	0.071	blend?
cep058	7.4089	20.721	0.058	20.507	0.084	
cep059	7.3858	20.736	0.058	20.296	0.068	
cep060	7.2814	20.722	0.066	20.339	0.066	
cep061	7.25995	19.699	0.051	19.318	0.065	blend?
cep063	7.15940	20.490	0.057	20.304	0.136	
cep064	7.13061	20.767	0.063	20.297	0.064	
cep066	6.8511	20.586	0.088	20.278	0.063	
cep067	6.8294	21.114	0.108	20.688	0.067	
cep068	6.6932	20.647	0.081	20.343	0.052	
cep069	6.6735	19.989	0.040	19.183	0.041	blend?
cep072	6.4250	20.742	0.058	20.263	0.069	
cep073	6.3065	20.809	0.067	20.395	0.060	
cep074	6.2719	20.915	0.080	20.517	0.076	
cep075	6.2713	20.806	0.091	20.425	0.074	
cep076	6.16368	20.896	0.068	20.517	0.075	
cep077	6.1329	21.025	0.093	20.438	0.081	
cep078	6.1098	21.151	0.091	20.858	0.127	
cep079	6.0795	20.861	0.126	20.471	0.069	
cep080	6.0749	20.919	0.081	20.582	0.081	
cep084	5.9343	21.042	0.090	20.730	0.122	
cep088	5.5369	19.677	0.036	18.680	0.032	
cep090	5.4844	21.052	0.079	20.450	0.069	

Table 2—Continued

ID	P	$\langle J \rangle$	$\sigma_{\langle J \rangle}$	$\langle K \rangle$	$\sigma_{\langle K \rangle}$	Remarks
cep092	5.39909	21.227	0.060	20.595	0.083	
cep094	5.2442	21.317	0.104	20.780	0.072	
cep095	5.2420	20.262	0.058	19.639	0.060	
cep096	5.2163	20.620	0.063	20.670	0.083	
cep097	5.17264	20.922	0.063	20.584	0.082	
cep098	5.0493	20.405	0.048	19.831	0.053	
cep099	5.03650	20.800	0.082	20.452	0.073	
cep100	4.9883	21.523	0.091	20.776	0.104	
cep101	4.9221	21.259	0.078	20.557	0.099	
cep102	4.7765	–	–	20.980	0.125	
cep103	4.5808	21.053	0.090	20.852	0.091	
cep104	4.5658	20.758	0.052	19.281	0.191	
cep105	4.5120	20.787	0.073	20.466	0.094	
cep108	4.0877	21.589	0.099	21.281	0.087	
cep110	3.9641	20.776	0.070	20.399	0.087	

Table 3. Previous and present distance determinations to NGC 3109

Reference	$(m-M)_0$	Errors	Method	Wavebands
Demers et al. (1985)	25.98	±0.15	Cepheids	*VR* (photographic)
Elias & Frogel (1985)	25.34	±0.1 (random)	M supergiants	*JHK*
Sandage & Carlson (1988)	26.0		Cepheids	*B* (photographic)
Capaccioli et al. (1992)	25.5	±0.2	Cepheids	*BV*
Richer & McCall (1992)	25.96	$^{+0.1}_{-0.4}$	planetary nebulae	narrow bandwidth
Lee (1993)	25.45	±0.15	TRGB	*I*
Musella et al. (1997)	25.67	±0.16	Cepheids	*BVRI*
Minniti et al. (1999)	25.62	±0.1	TRGB	*I*
Karachentsev et al. (2002)	25.62	±0.13	TRGB	*I*
Méndez et al. (2002)	25.52	±0.06 (internal) ±0.18 (systematic)	TRGB	*I*
this paper	25.57	±0.02 (random) ±0.06 (systematic)	Cepheids	*VIJK*

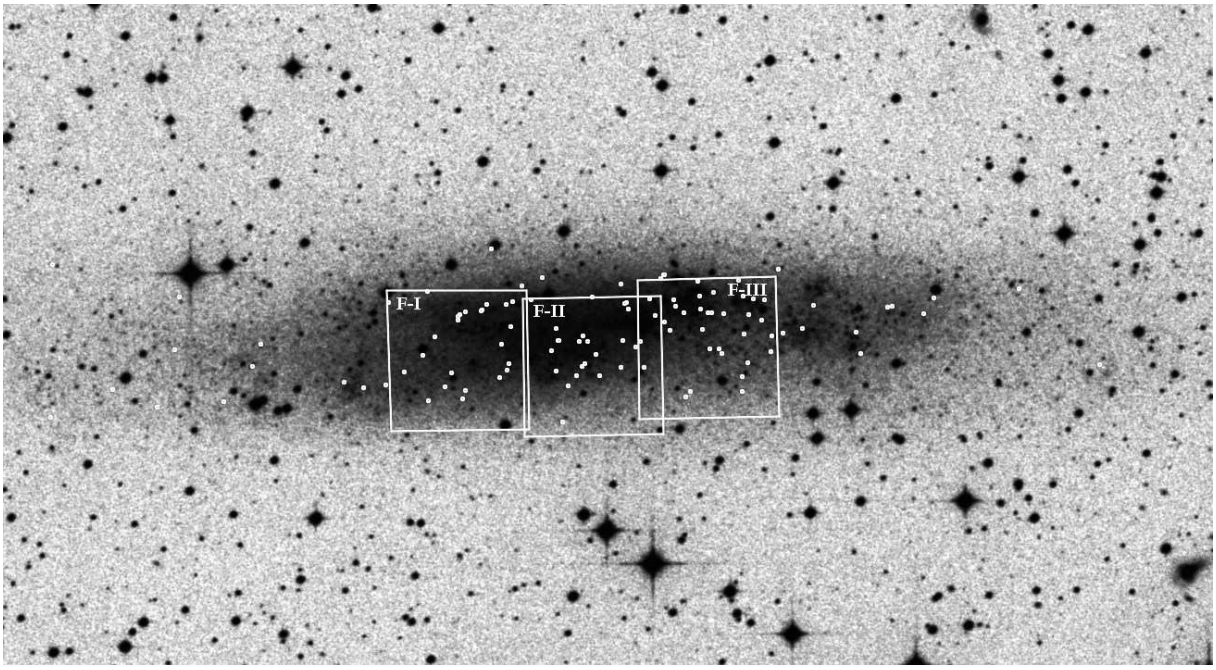

Fig. 1.— Contours of the observed fields in NGC 3109 on the DSS-2 red plate. White points mark the Cepheids reported in Paper I.

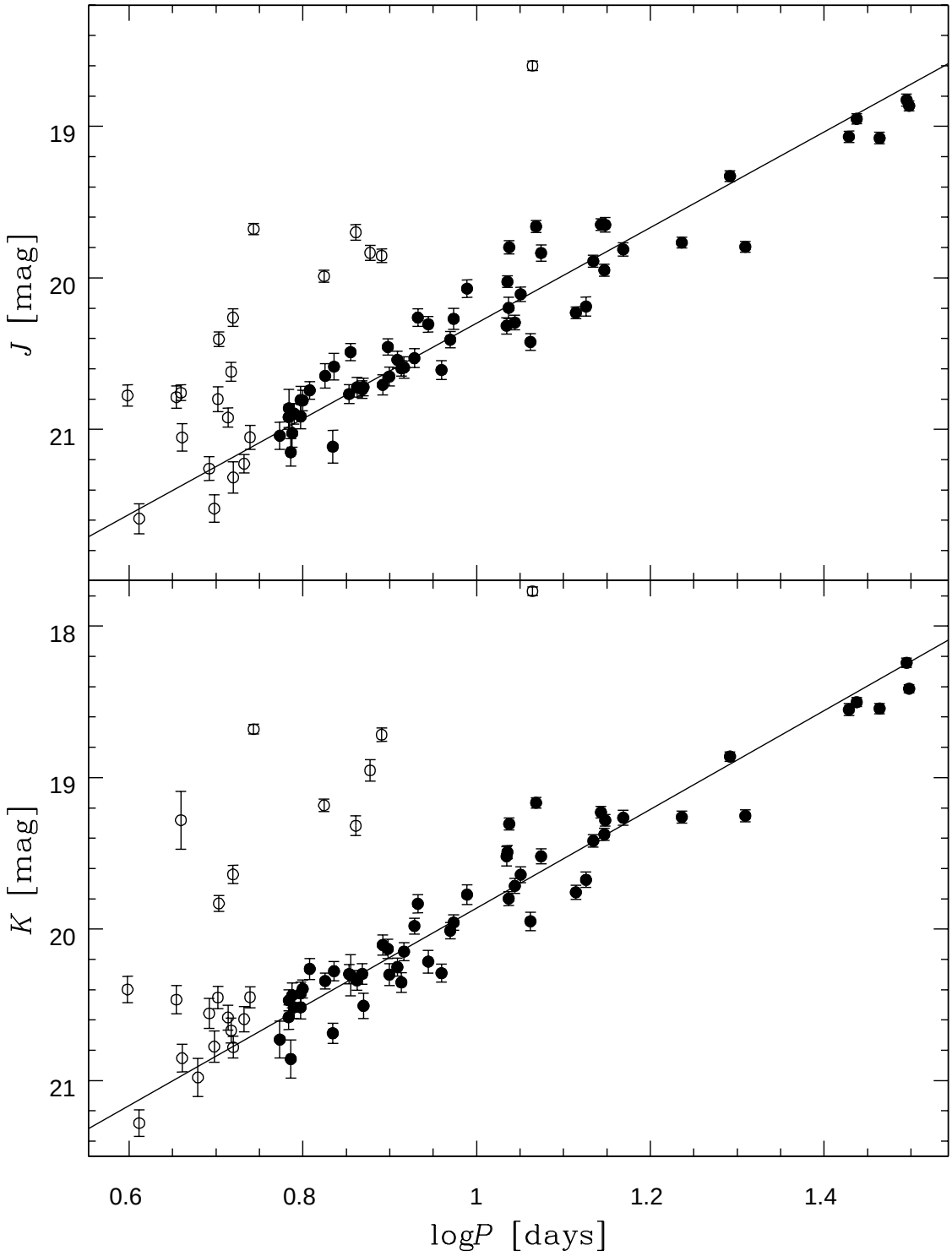

Fig. 2.— J- and K-band PL relations for Cepheids in NGC 3109. The straight lines are the linear least-squares fits to the points marked with filled circles. In both diagrams, we adopted the slopes derived by Persson et al. for the LMC Cepheids. The empty circles are short-period and outlying Cepheids omitted from the fit (see text).

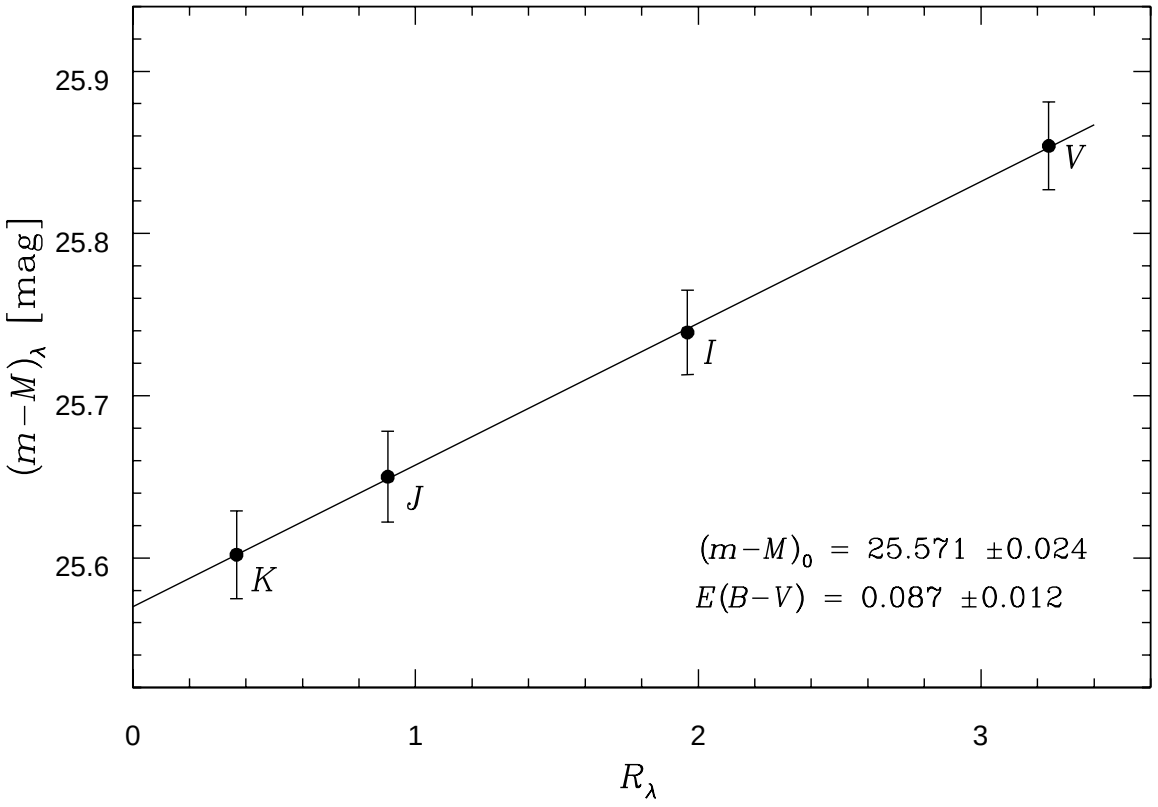

Fig. 3.— Apparent distance moduli to NGC 3109 determined in different photometric bands, versus the ratio of total to selective absorption for these bands. The intersection and slope of the best-fitting line gives the true distance modulus and the total color excess, respectively.

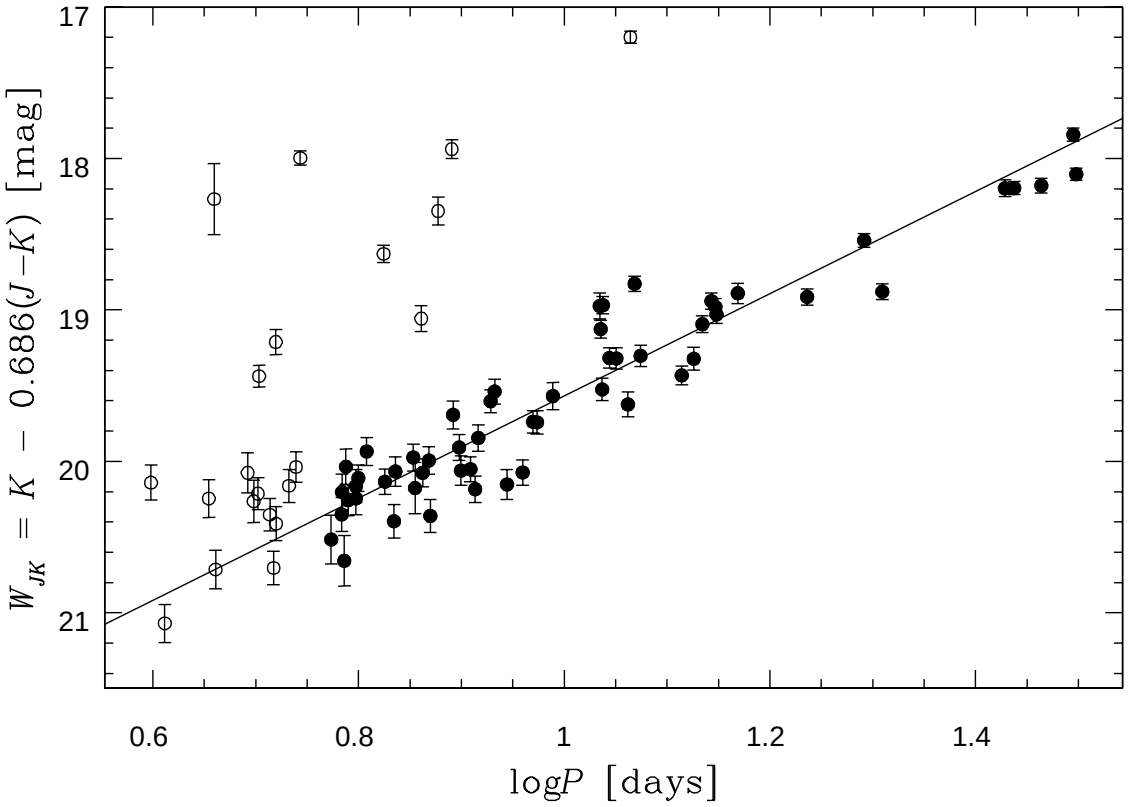

Fig. 4.— The period – NIR Wesenheit index diagram for Cepheids in NGC 3109. The line shows the linear least-squares fit to the points indicated by filled circles, adopting the slope derived from the LMC Cepheids. The empty circles are short-period and outlying Cepheids omitted from the fit.

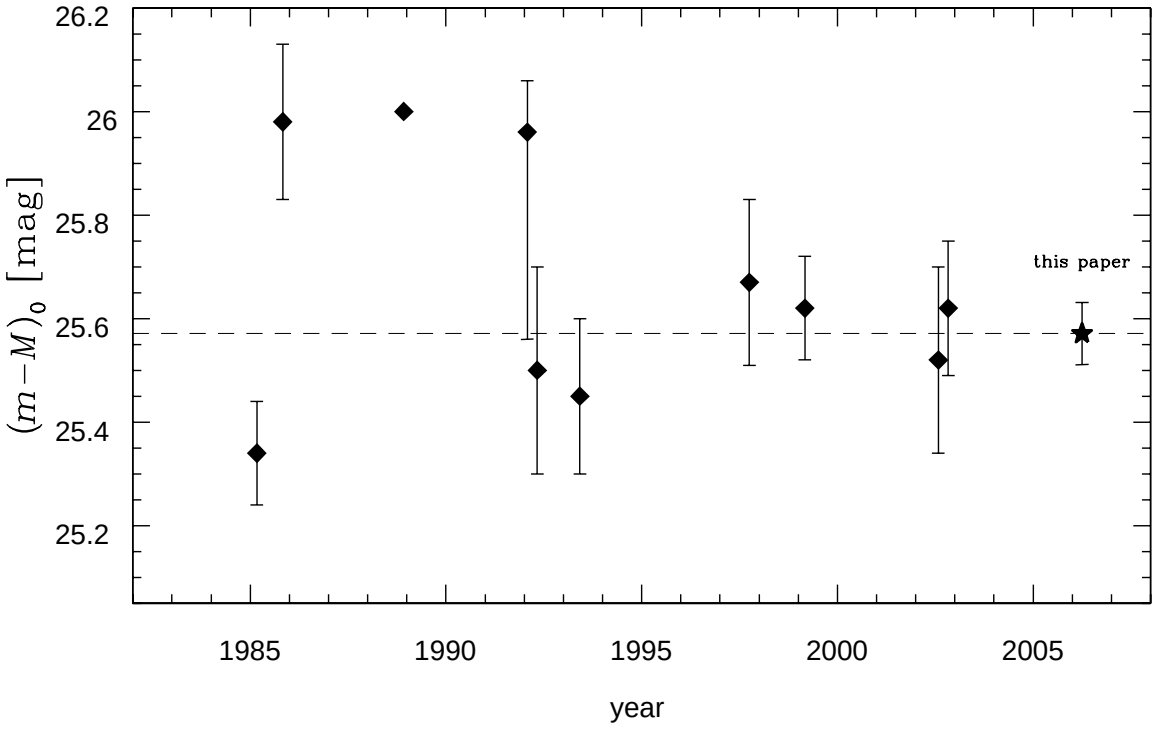

Fig. 5.— Previous distance determinations to NGC 3109 (diamonds) in comparison to our present determination (star). Numerical values and techniques used for the individual determinations are given in Table 3.